JSES International 6 (2022) 748–754

Contents lists available at ScienceDirect

JSES International

journal homepage: www.jsesinternational.org

What is the best position for coracoid fixation in the Latarjet procedure?

Guilherme Augusto Stirma, MD[a,*], Leandro Massini Ribeiro, MD[a], Evandro Dias Gaio[b], Paulo Santoro Belangero, PhD[a], Eduardo Antonio de Figueiredo, PhD[a], Alberto de Castro Pochini, PhD[a], Carlos Vicente Andreoli, PhD[a], Benno Ejnisman, PhD[a]

[a]*Federal University of São Paulo, Paulista School of Medicine - UNIFESP, São Paulo (SP), Brazil*
[b]*Federal University of Juiz de Fora, Minas Gerais, Brazil*

ARTICLE INFO

Keywords:
Latarjet
Failure strength
Numerical models
Finite element analysis
Coracoid geometric
Screws

Level of evidence: Basic Science Study; Computer Modeling

Hypothesis: Multiple problems and complications associated with Latarjet fixation have been described; thus, this is the first study in the literature to identify the maximum allowed screw clamping force and best fixation screw position for Latarjet surgery.

Methods: A variation of distal and proximal coracoid screw positions with and without a flat washer was evaluated through finite element analysis, at a minimum distance of 3 mm from the edge. A loading progression test was performed until the maximum stress reached a limit imposed by the bone yield. We identified the maximum allowed screw clamping force based on a von Mises and maximum principal stresses failure theory.

Results: When using the flat washer, the cortical bone generally has only space for 1 piece. For this reason, as a primary study, it was observed that when the distal screw was more than 7 mm from the edge, the clamping force supported will be higher than that during the proximal fixation regardless of the proximal location screw. We have found that the best position is 7 mm from the distal edge, with the highest compression of 445 N (7 mm proximal distance, 5 mm distal distance) in due respect to the von Mises failure theory. To get around this lack of space situation, in this study, we have proposed a fixation plate to replace the flat washer. This plate has shown very interesting values when compared to the previously flat washer study, but now, for both screw holes. With those results, we can assure that using a fixation plate like this will ensure surgery safety and higher allowed compression force when clamping the bolts.

Conclusion: The distal screw provided higher tensile strength values when located more than 7 mm from the coracoid edge. The geometry of the coracoid in its distal position supports higher stress loads than in the proximal position. When the flat washer was in the proximal position, the coracoid was submitted with a more distributed and uniform load, preventing localized bone damage as a crush.

In the original surgery technique by Dr. Michel Latarjet, which is the standard treatment for recurrent anterior instability of the shoulder with bone loss, the coracoid process is fixed with 1 screw on the anteroinferior glenoid border.[18] Since then, the original procedure has been modified and improved based on biomechanical research studies. With regard to fixation devices, methods using 2 screws, interference screws, and plating have been proposed.[13] Stable fixation with maximum compression is essential to avoid acute and chronic complications; however, it is crucial not to break the coracoid process during screw fixation.[4]

Good compression of the bone block is mandatory to achieving successful outcomes. Screw strength and length are important as long screws may cause nerve injuries and short ones may result in insufficient compression, nonunion, and coracoid process migration.[5,6,13]

In the technique described by Watch and Boileau,[2] 2 malleolar screws were used without a specified distance between them or to the proximal and distal margins of the bone. The drilling position in the graft has great importance and can increase the risk of graft fracture during preparation and glenoid fixation.[2]

Since 1970, the number of publications related to bone load analysis, arthroplasties, and osteosynthesis has increased.[8,14] The

Institutional review board approval was not required for this study.
This work was developed by the Federal University of São Paulo (UNIFESP) Department of Orthopedics and Traumatology—Sports Traumatology Center (CETE).

*Corresponding author: Guilherme Augusto Stirma, MD, Federal University of São Paulo, Paulista School of Medicine - UNIFESP, Street Arruda Alvim, número 297, Ap 205, São Paulo, Brazil.
E-mail address: Drstirma@outlook.com (G.A. Stirma).

https://doi.org/10.1016/j.jseint.2022.05.008

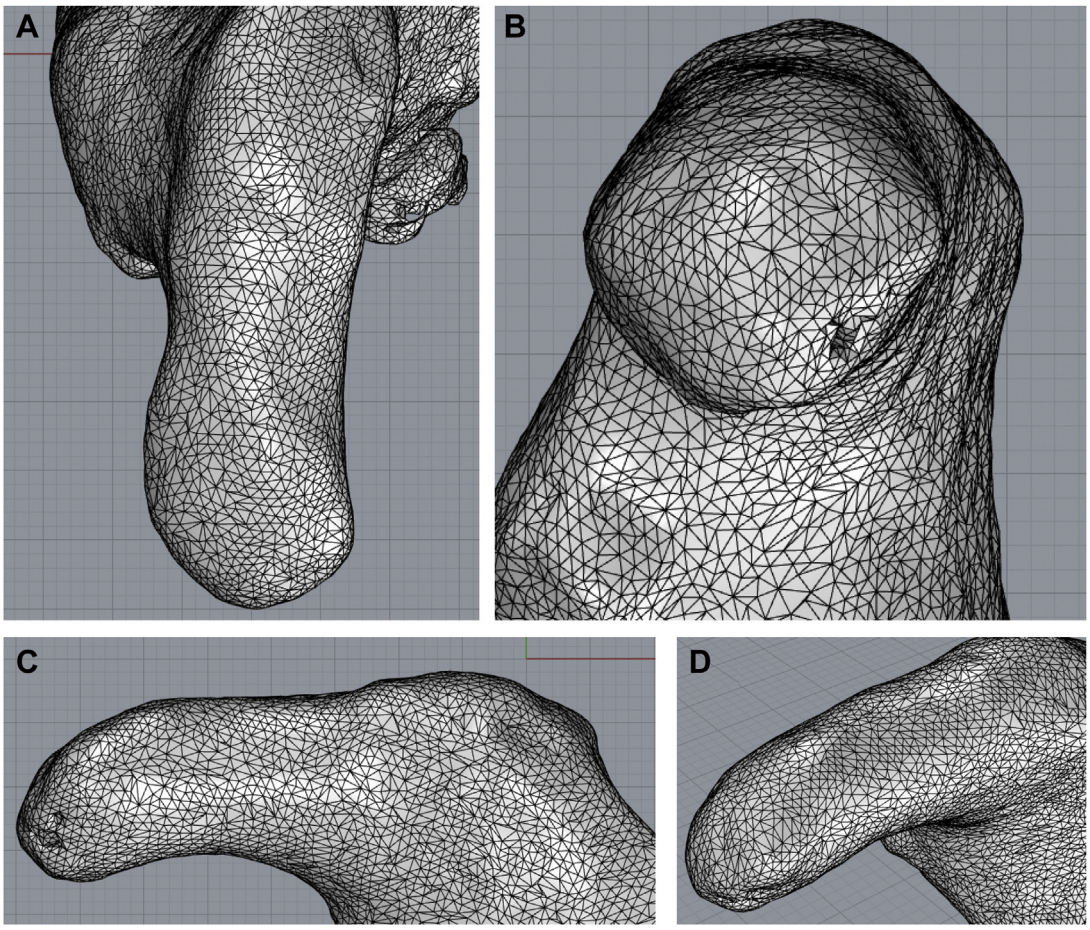

Figure 1 Virtual geometric three-dimensional (3D) model used to build a 3D coracoid model. (**A**) Top, (**B**) front, (**C**) right, (**D**) perspective view.

stress analysis of bones by the *solid mechanics theory* enhanced with numerical models is key to assess fracture risk and design fracture fixation.[7] The finite element analysis (FEA) can be used to evaluate the effects of a load on the bone (irregular geometries and heterogeneous material properties) as well as its biomechanical behavior.

The development of subject-specific finite element (FE) models from computed tomography data is a powerful tool to nondestructively investigate bone strength in vivo: Actually, subject-specific FE models are capable to include most of the internal parameters which contribute to bone strength and simulate the influence of general and variable external boundary conditions.[16]

The purpose of our study is to identify the maximum allowed screw clamping force to avoid the intraoperative coracoid fracture. The ductile failure theory of von Mises was chosen to evaluate the fracture fail risk due to its wide application and flexibility in the fracture mechanics field. This method relates the normal and shear stresses provided by a load, which in our case is the force applied in the screw, with the maximum stress allowed by the material, which in our case is the yield stress of the bone.

Materials and methods

Subject-specific geometries/who were undergoing the Latarjet procedure?

Computed tomography was used to determine cortical coracoid thickness in 10 patients between 20 and 30 years of age preoperative to the Latarjet procedure. Series of orthogonal short-axis and long-axis images were acquired. The short-axis images were of 1.1-mm pixel size, and each short-axis slice was separated by 2 mm. In the middle of the distance from the distal (coracoid tip) and proximal (osteotomy) coracoid, we analyzed the sagittal, axial, and coronal planes to calculate the cortical coracoid thickness ([sagittal + axial + coronal]/3). The cortical thickness average value achieved, 3 planes listed for 10 patients, was 1.875 cm.

Afterwards, Rhino 6 software (Rhinoceros; Robert McNeel & Associates, Seattle, WA, USA) was used for designing a 3D coracoid model (Fig. 1). The size and dimensions of the 3D coracoid model were based on a review by Alves et al.[1] The coracoid dimensions of the grafts were the same regardless of the gender; the mean length, thickness, and width were 22.6, 7.9, and 14.0 mm, respectively, for 31 patients.[2] Two partially threaded 4.0-mm screws were created with a cylindric head (6.0 mm). The flat washer had a diameter of 1.0 cm (Fig. 2). The glenoid was represented using a solid box (20.0 × 14.0 × 2.0 mm—length × width × thickness) and used as a fixed support and to make contact with the entire extension, inferior face, of the coracoid (Fig. 3); the miniplate dimension was 22.6 × 7 × 2 mm (length × width × thickness) with 2 central holes of 4.0-mm diameter (Fig. 4).

Computational modeling

The entire study was conducted through FEA (Fig. 3)[14] to calculate the mechanical response of the bone and plate in each

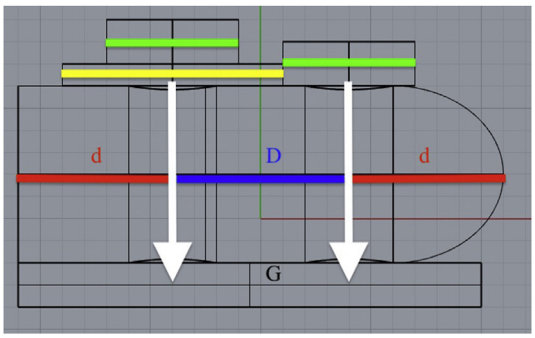

Figure 2 Representative figure of the 2D drawing for the positioning of the screws and the coracoid. *d*, Distance to edge; *D*, distance between the screws; *G*, glenoid. *Green color*, screw; *yellow color*, flat washer; *white arrows*, fixation direction.

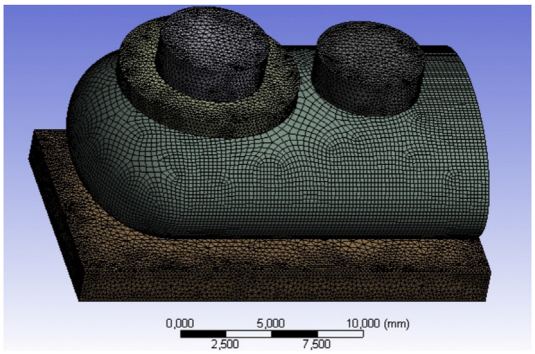

Figure 3 Three-dimensional coracoid model with coracoid mesh to finite element method.

scenario. The numerical models were implemented using the FEA software Ansys, version 19.2 (Canonsburg, PA, USA), and calculated on a *Pentium I7 10th-generation* computer (Santa Clara, CA, USA).

Loading scenarios and screw locations

Possible screw locations in the coracoid were decided. The minimum distance from the distal (coracoid tip) and proximal (osteotomy) coracoid graft was 3 mm (screw head with a radius of 3 mm) and 8 mm, respectively, between the holes for fixation (3 mm from the screw head and 5 mm from the flat washer; Fig. 2). The angles for fixing were 0° (parallel), and the type of force used was compression. All screw positions were tested with flat washers in the proximal and distal screws.

We evaluated the force application in different coracoid positions and directions to predict biomechanical responses (Fig. 2). The compression load progressed until a maximum limit, lower than the bone yield strength. It was defined through pretensioning with friction, allowing the phenomenon of friction between the screw and the bone to be considered.

Mechanical contact behavior

The flat washer, screw head, and the superior coracoid cortical bone, as well as the glenoid, were in total contact with the inferior coracoid cortical bone. A statistical mesh analysis and a mesh convergence study were performed[4] in order to use the Tresca friction contact behavior, which is responsible to represent both rotational dynamics and crush contact.[19] The Newton method was used to linearize the equations.

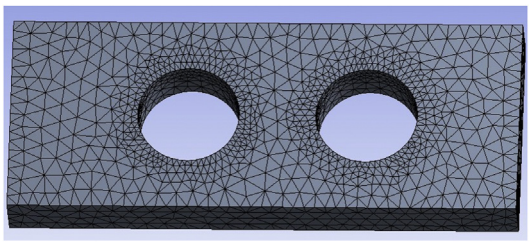

Figure 4 Miniplate. Coracoid stresses topology optimization (TO) study generated by the clamping force of the proximal and distal screw. The density of lines presents the areas of greater detail for mathematical study.

Table I
All property values used for finite elements tests in cortical bone

Young's modulus (Ey)	1.15E10 Pa
Young's modulus (Ez)	1.70E10 Pa
Poisson's ratio (νxy)	0.51
Poisson's ratio (νyz)	0.31
Poisson's ratio (νxz)	0.31
Shear modulus (Gxy)	3.6E9 Pa
Shear modulus (Gyz)	3.3E9 Pa
Shear modulus (Gxz)	3.3E9 Pa
Yield strength (MPa)	129.814

Constitutive and material laws

This step is fundamental for differentiating among mechanical problems in general as the use of a material law describing the correct study-case stress-strain relationship, additional information if necessary, and appropriate boundary conditions must be prescribed to configure this specific study.

Since cortical bone represents nearly 80% of the skeletal mass and there is a “grain” or preferred direction and Young's modulus varies with that direction,[16] the material law used for the bone is orthotropic, and all property values used in this study were obtained from the literature (Table I). The yield strength used is for cortial bones in young patients.[10]

The mesh was developed using the concept of a thin-walled structure as the thickness of the model is small relative to the length and width, and this allows the use of a simplified analysis through shell elements. Isoparametric elements with 2 degrees of freedom at each node and impeding translations perpendicular to the plane guarantee a plan state analysis.

Failure criterion

The primary requisites for the failure criterion to be implemented in the FE models are to reproduce to the maximum extent possible the elastic limit behavior observed experimentally for bone tissue, being as simple as possible to implement.[11] A maximum principal strain criterion and the theory of maximum distortion energy, including asymmetry in the tensile/compressive limit values, were selected because they incorporate many of the fundamental bone elastic limit characteristics reported in the literature: isotropy in mono-axial loading conditions and invariance with respect to density. To guarantee the validity of our model, deformations were also verified for each case, maintaining the hypothesis of small deformations of the constitutive model.

Results

The principal stress distribution is presented in megapascals for the coracoid simulation models, and its magnitude is shown at the

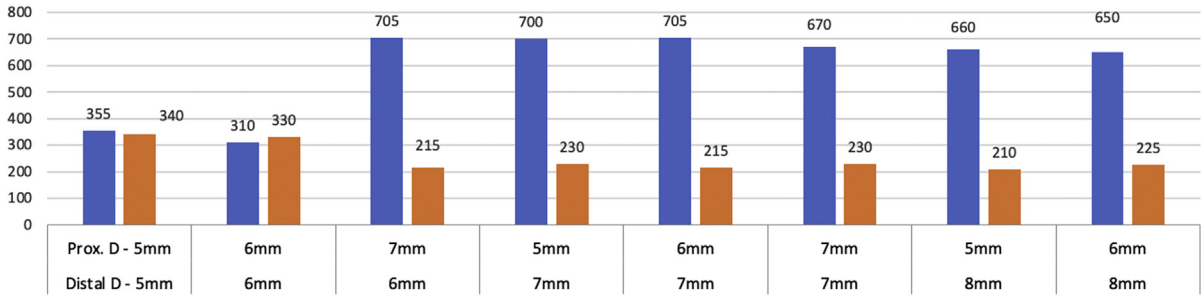

Figure 5 Distal hole with flat washer vs. proximal hole without flat washer—bars show graphical distribution. *Prox. D*, proximal distance; *Distal D*, distal distance. *Blue color*, distal hole with flat washer, N/mm (screw clamping force); *orange color*, proximal hole without flat washer, N/mm (screw clamping force).

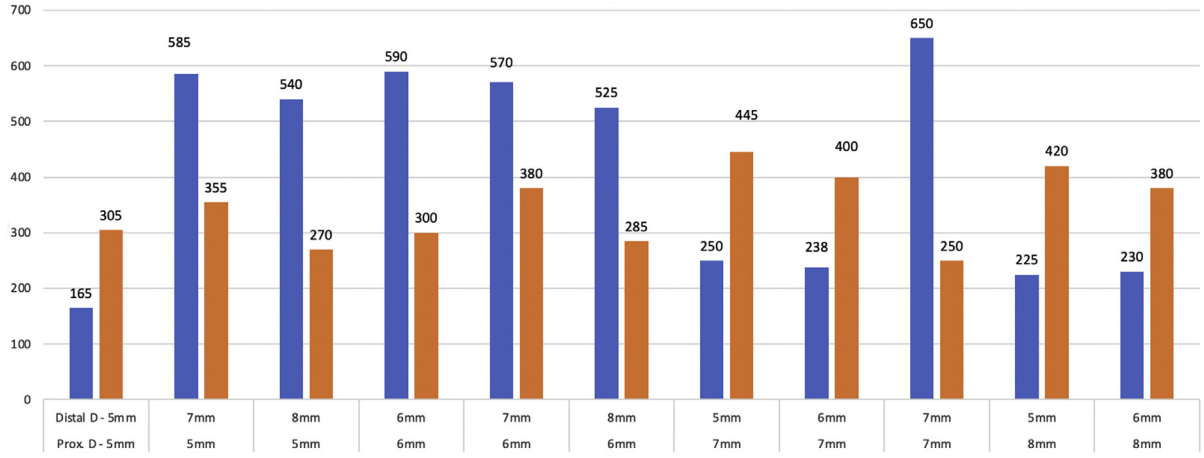

Figure 6 Proximal hole with flat washer vs. distal hole without flat washer—bars show graphical distribution. *Distal D*, distal distance; *Prox. D*, proximal distance. *Blue color*, distal hole without flat washer, N/mm (screw clamping force); *orange color*, proximal hole with flat washer, N/mm (screw clamping force).

colored bar. These are the von Mises stresses that are used with the maximum distortion energy theory to evaluate whether the material will fail due to static loads.

The coracoid geometric distal part (conjoined tendon insertion) has an oval shape. Looking at the stress-strain distribution, we may see a less deformed area when the same load was applied. Therefore, it is conclusive that a higher force may be applied at the distal position than at the proximal one.

The best advantage of using a flat washer is the load distribution from the concentrated load of the bolt's head to the bone, avoiding punctual damage, fracture, or other kinds of failures. Furthermore, we are only able to use 1 flat washer because of the lack of space. For this reason, it is more useful to keep the flat washer fixed at the distal position since it supports a higher compression force. Figure 5 represents the variation of the possible position for both holes at the available coracoid space. Through this study, respecting the von Mises failure theory, we found the highest compression load value of 705 N/mm at the distal position (6 mm proximal distance and 7 mm distal distance) to keep the bone free of static failure. There was a significant increase in the applied force when the hole with a screw and flat washer in the distal portion was located 7 mm from the distal edge, regardless of the proximal screw. So we can conclude that the use of a flat washer, mainly at this best position, induces a significant increase of force that can be applied or, even for the same load, a higher safety coefficient.

In the interpretation of the distribution, it was observed that when the distal screw was above 7 mm from the edge, it had a force higher than the proximal fixation regardless of the proximal location screw. When the distal screw was close to the edge (6 mm and 5 mm), the proximal screw location with a flat washer exhibited higher fixation, with the highest tension being 445 N (7 mm proximal distance and 5 mm distal distance) (Fig. 6).

The average values for fixation force with a flat washer at proximal and distal locations were similar in both cases for every tested position (Fig. 7). In another hand, there was a significant increase in the allowed strength when the screws located in the distal portion were 7 mm from the edge, regardless of the position of the flat washer. The location of the screw in the proximal portion did not interfere with the result of the average force.

In the final analysis, Figure 8 demonstrates the developed plate after a topological optimization. This new model was generated for a low-cost construction by using the essence of the analyzed results as an input. Additionally, it observes a more homogeneous distribution of stresses than with models of the fixation plate. The previous plate was 22.6 mm long, resulting in complete coverage of the coracoid graft. Since the magnitude of applied forces were equivalent at both screw fixation points, the maximum allowed compression forces were generated for fixation at 7 mm of the proximal edge and 7 mm of the distal edge, reaching an average value of 410 N; 8 and 6 mm, with 432 N; and 9 and 5 mm, with 430 N (Fig. 9).

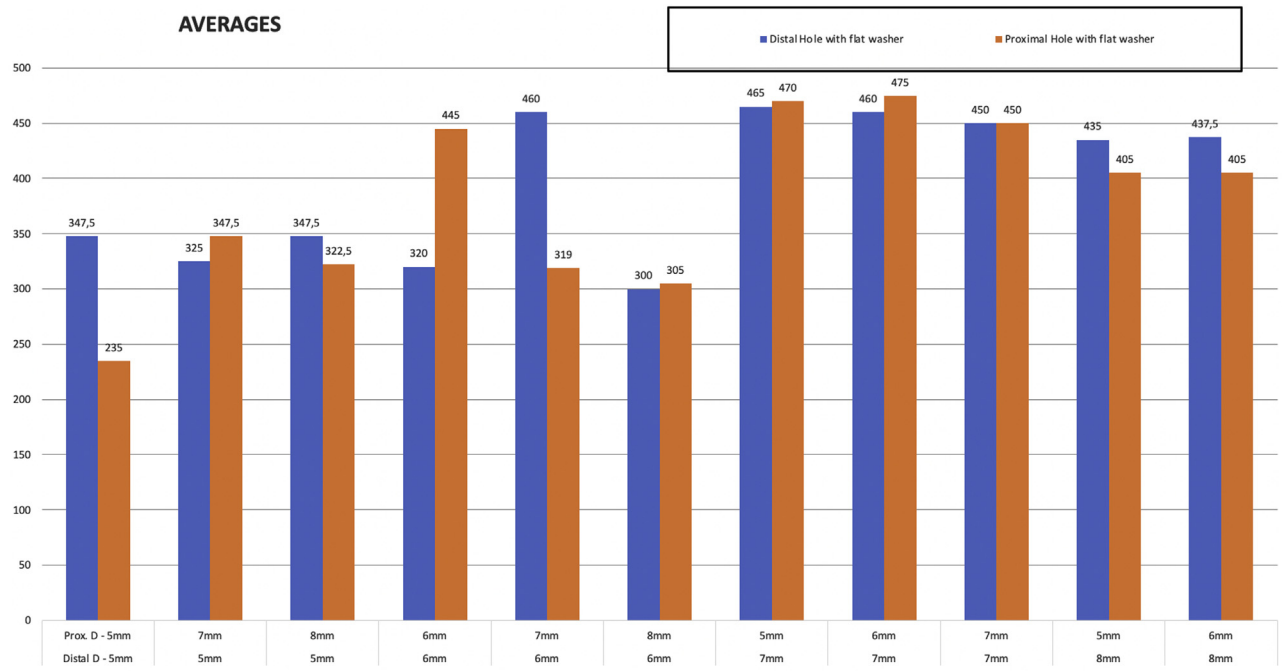

Figure 7 Average tension ([proximal screw clamping force + distal screw clamping force]/2). *Prox. D*, proximal distance; *Distal D*, distal distance. *Blue color*, distal hole with washer, N/mm (screw clamping force); *orange color*, proximal hole with washer, N/mm (screw clamping force).

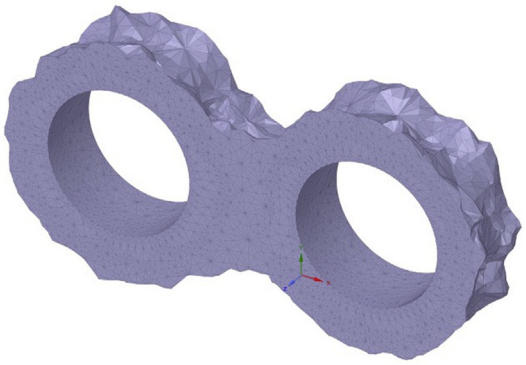

Figure 8 Stresses in the model with a fixation plate. Homogeneous distribution of stresses in the model (same tension in proximal and distal hole).

Discussion

In the open or arthroscopic Latarjet technique, 2 bicortical screws are commonly used as a fixation method. However, screw fixation is also a source of complications,[2] which include nonunion, neurovascular damage, screw migration, loosening, fixation position, and the most important, the fracture of the coracoid graft being intraoperative.[6] Comparative data on the biomechanical behavior of cortical buttons, fixation of the interference screw, and fixation of the screw during the Latarjet-Bristow procedure are frequently reported in the literature. However, this is the first study aiming to identify the best location, minimum distance, and safe distance to avoid graft fracture. We used the classic Latarjet technique graft position in the glenoid, simulated with 2 screws—4.0-mm cancellous screws—with three possibilities—flat washers in the proximal, distal position, or a miniplate in almost all possible fixation locations in the coracoid graft. The main function of the flat washer is to increase the screw contact, as it is known that the higher the contact area between the screw and the surface, the better the distribution of the applied force and the stronger the fixation. Giles et al studied strength and joint contact in classic Latarjet coracoid transfer and compared it with the congruent arc technique.[3,4] Biomechanical tests showed improved fixation stability and strength with the classic Latarjet technique.[4] Shin et al, in a biomechanical study with 35 fresh-frozen cadaveric shoulders, showed that the screw type or fixation method does not significantly influence the properties of fixation in the classic Latarjet procedure. The authors used 2 screws, and the screws included were partially threaded solid 4.0-mm cancellous screws, solid 4.0-mm cancellous screws with unicortical fixation, fully threaded solid 3.5-mm cortical screws, total threaded cannulated 4.0-mm cancellous screws, and partially threaded cannulated 4.0-mm screws. These findings suggest that surgeons may continue to select screws and fixation methods based on choice without significantly compromising the biomechanical properties. There were no differences between different screw types or fixation methods after cyclic loading or in loading to failure during the failure test.[12,13] Frank et al suggested that the angle of screw insertion was linked with biomechanical outcomes and obtained lower maximum loads to failure and higher displacement with screws fixed at 15° than for constructs with screws inserted at 0° (where 0° represents an insertion angle perfectly perpendicular to the bone).[3] In the present study, the screws were fixed at an angle of 0°.

In research and projects in orthopedics, there is an increasing use of mathematical models as an instrument to analyze the effects of stresses on bones subjected to forces. The bone shape and physical properties are built by computation with software programs, and physical interactions are calculated in terms of stresses and deformations.[3] Additionally, simplifications in mathematical models can enable complex analyses.[15] The finite element method modeling analysis results of bones depend on the anatomical location, cortical thickness, anisotropic material properties, and bone mass.[7] The finite element method considers the structures to be small particles of finite quantity connected to a finite number of

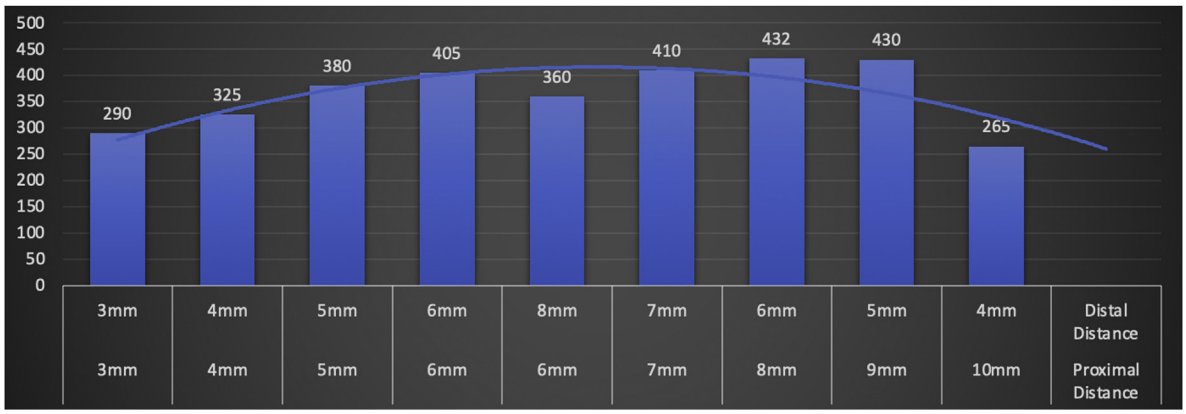

Figure 9 Plate tension. Bars show graphical distribution. Compression forces in proximal distance and distal distance at the coracoid edge.

points, called nodes or nodal points. It is possible to evaluate the distribution of stresses in a structure observing the deformation or visualizing and interpreting the images.[14] This coupled model represents a more realistic phenomenon showing results in agreement with biomechanical tests[9,13]; however, the problem becomes nonlinear, and the mesh and solution of the differential equations require more attention.

Analyzing the fixation with screws and flat washers, it was observed that the flat washer in the proximal position presented a lower difference in the load between the screws. The anatomy of the coracoid allows the distal graft portion to absorb higher force; thus, when fixing the screw with a flat washer in the proximal position, there is a tendency for better force distribution, as even without the flat washer, the screw in the distal position obtained higher applied force (Fig. 5). When the flat washer was placed in the distal position, the difference in load to failure between the 2 screws was higher, particularly when the screw was fixed at 7 mm or 8 mm from the distal border.

Our study showed a higher difference between the compressive force at the 2 sites and that the minimum distance to achieve a higher load for distal screw fixation to the distal edge was 7 mm (with or without flat washer, $P = .01$), but there was no statistical difference when analyzing the distance to proximal screw fixation.

The most homogeneous results were in the miniplate, which allowed improved stress distribution because of the larger surface area of the plate compared with flat washers or screw heads alone. The miniplate was 20 mm long as the miniplate was out of contact with 2 mm in the distal position because of the distal coracoid geometry. Tests to achieve the best location on the miniplate have shown that the positioning of the screws tends to be closer to the distal edge associated with the shortest possible distance between the 2 screws, that is 6 mm.[17] We believe that the plates, due to its better stress distribution, could be a mechanical factor that prevents graft resorption. However, clinical studies are lacking for this conclusion.

This study has several limitations, including the use of mathematical biomechanical models as alternatives to cadaveric specimens. We chose software to maintain bone uniformity and excluded the effect of the difference in bone quality and density. In addition, the geometry and surface were designed in software programs to simulate real conditions. In this mathematical study, we were able to design perfect contact of the bone block against the glenoid, which is not always true in real cases. The values for the simulation and coracoid design are averages. The glenoid was created as a flat surface to obtain all contacts with the coracoid. However, in surgical procedures, this contact is often not reached. The geometry of coracoid process was determined as perfectly symmetric. Individual differences of bone morphology constitute one of the important pathogenetic factors of intraoperative fracture.

Conclusion

We obtained higher tensile strength values for the distal screw positioned 7 mm above the coracoid edge. The geometry of the coracoid in its distal position supports higher stress loads than in the proximal position. The flat washer improved force distribution, allowing higher application of force in the fixation. Based on the results, the miniplate has better force distribution, and the flat washer in the distal position exhibited a considerable difference in strength when compared to the proximal flat washer. Thus, the flat washer in the proximal position provided a more uniform distribution of forces. More uniform the forces, the lower the tension and risk of fracture.

Disclaimers:

Funding: No funding was disclosed by the authors.
Conflicts of interest: The authors, their immediate families, and any research foundation with which they are affiliated have not received any financial payments or other benefits from any commercial entity related to the subject of this article.

References

1. Alves BV, Silva GS, Matsumoto FY, Ferreira MT, Britto AG, Mothes FC. Comparative Evaluation of Coracoid Graft Dimensions in the Latarjet Surgery for Anterior Glenohumeral Instability. Rev Bras Ortop (Sao Paulo) 2020;55:215-20. https://doi.org/10.1055/s-0039-1698801.
2. Boileau P, Saliken D, Gendre P, Seeto BL, D'Ollonne T, Gonzalez JF, et al. Arthroscopic Latarjet: suture-button fixation is a safe and reliable alternative to screw fixation. Arthroscopy 2019;35:1050-61. https://doi.org/10.1016/j.arthro.2018.11.012.
3. Frank RM, Roth M, Wijdicks CA, Fischer N, Costantini A, Di Giacomo G, et al. Biomechanical analysis of plate fixation compared with various screw configurations for use in the Latarjet procedure. Orthop J Sports Med 2020;8:1-6. https://doi.org/10.1177/2325967120931399.
4. Giles JW, Puskas G, Welsh M, Johnson JA, Athwal GS. Do the traditional and modified Latarjet techniques produce equivalent reconstruction stability and strength? Am J Sports Med 2012;40:2801-7. https://doi.org/10.1177/0363546512460835.
5. Hardy A, Gerometta A, Granger B, Massein A, Casabianca L, Pascal-Moussellard H, et al. Preoperative CT planning of screw length in arthroscopic Latarjet. Knee Surg Sports Traumatol Arthrosc 2018;26:24-30. https://doi.org/10.1007/s00167-016-4286-8.
6. Kazum E, Chechik O, Pritsch T, Mozes G, Morag G, Dolkart O, et al. Biomechanical evaluation of suture buttons versus cortical screws in the Latarjet – Bristow procedure: a fresh - frozen cadavers study. Arch Orthop Trauma Surg 2019;139:1779-83. https://doi.org/10.1007/s00402-019-03269-6.

7. Parashar SK, Sharma JK. A review on application of finite element modelling in bone biomechanics. Perspect Sci 2016;8:696-8. https://doi.org/10.1016/j.pisc.2016.06.062.
8. Pécora JOR, Neves Junior AT, Roesler CRM, Fancello EA, Malavolta EA, Gracitelli MEC, et al. Glenoid track evaluation by a validated finite-element shoulder numerical model. Revue de Chirurgie Orthopedique et Traumatologique 2020;106:413. https://doi.org/10.1016/j.rcot.2020.03.016.
9. Provencher MT, Aman ZS, LaPrade CM, Bernhardson AS, Moatshe G, Storaci HW, et al. Biomechanical comparison of screw fixation versus a cortical button and self-tensioning suture for the Latarjet procedure. Orthop J Sports Med 2018;6:1-7. https://doi.org/10.1177/2325967118777842.
10. Sanada JT. Avaliação Da Resistência E Módulo De Elasticidade De Osso Mineralizado E Desmineralizado Pelos Testes De Microtração. São Paulo, Brazil. 2007:112. https://doi.org/10.11606/D.25.2007.tde-19062007-133051.
11. Schileo E, Taddei F, Cristofolini L, Viceconti M. Subject-specific finite element models implementing a maximum principal strain criterion are able to estimate failure risk and fracture location on human femurs tested in vitro. J Biomech 2008;41:356-67. https://doi.org/10.1016/j.jbiomech.2007.09.009.
12. Schmiddem U, Hawi N, Liodakis E, Dratzidis A, Kraemer M, Hurschler C. Monocortical fixation of the coracoid in the Latarjet procedure is significantly weaker than bicortical fixation. Knee Surg Sports Traumatol Arthrosc 2018;27:239-44. https://doi.org/10.1007/s00167-018-4837-2.
13. Shin JJ, Hamamoto JT, Leroux TS, Saccomanno MF, Jain A, Khair MM, et al. Biomechanical analysis of Latarjet screw fixation: comparison of screw types and fixation methods. Arthroscopy 2017;33:1646-53. https://doi.org/10.1016/j.arthro.2017.03.030.
14. Soni JF, Santili C, Lancellotti CLP, Hecke MB, Almeida FR de, Karam LZ. Análise comparativa em modelo computadorizado bidimensional com simulação do emprego de hastes flexíveis de aço e titânio, na fratura do fêmur da criança, utilizando o método dos elementos finitos. Revista Brasileira de Ortopedia 2008;43:183-92. https://doi.org/10.1590/s0102-36162008000400005.
15. Terrier A, Vogel A, Capezzali M, Farron A. An algorithm to allow humerus translation in the indeterminate problem of shoulder abduction. Med Eng Phys 2008;30:710-6. https://doi.org/10.1016/j.medengphy.2007.07.011.
16. Turner CH, Cowin SC, Rho JY, Ashman RB, Rice JC. The fabric dependence of the orthotropic elastic constants of cancellous bone. J Biomech 1990;23:549-61.
17. Wu C, Zheng K, Fang J, Steven GP, Li Q. Time-dependent topology optimization of bone plates considering bone remodeling. Computer Methods Appl Mech Eng 2020;359, 112702. https://doi.org/10.1016/j.cma.2019.112702.
18. Young AA, Baba M, Neyton L, Godeneche A, Walch G. Coracoid graft dimensions after harvesting for the open Latarjet procedure. J Shoulder Elbow Surg 2013;22:485-8. https://doi.org/10.1016/j.jse.2012.05.036.
19. Zhang DW, Ou H. Relationship between friction parameters in a Coulomb-Tresca friction model for bulk metal forming. Tribology Int 2016;95:13-8. https://doi.org/10.1016/j.triboint.2015.10.030.